Received: 30 December 2016 | Revised: 9 February 2017 | Accepted: 10 February 2017

DOI 10.1002/cne.24191

RESEARCH ARTICLE

WILEY The Journal of Comparative Neurology

Select noxious stimuli induce changes on corneal nerve morphology

Deborah M. Hegarty | Sam M. Hermes | Katherine Yang | Sue A. Aicher

Department of Physiology and Pharmacology, Oregon Health & Science University, Portland, Oregon

Correspondence
Sue A. Aicher, Department of Physiology and Pharmacology, Oregon Health & Science University, Mail code: L334, 3181 Sam Jackson Park Road, Portland, OR 97239-3098, USA.
Email: aichers@ohsu.edu

Funding information
This work was supported by grants from the NIH: DE12640 (SAA, DMH, and SMH); P30 NS061800 (OHSU Neuroscience Imaging Center); shared instrumentation grant RR016858 (LSM 510 confocal microscope). SAA was also supported by OHSU Presidential Bridge funds. Support was also provided by Saturday Academy's Apprenticeships in Science and Engineering (ASE) program (KY).

Abstract

The surface of the cornea contains the highest density of nociceptive nerves of any tissue in the body. These nerves are responsive to a variety of modalities of noxious stimuli and can signal pain even when activated by low threshold stimulation. Injury of corneal nerves can lead to altered nerve morphology, including neuropathic changes which can be associated with chronic pain. Emerging technologies that allow imaging of corneal nerves in vivo are spawning questions regarding the relationship between corneal nerve density, morphology, and function. We tested whether noxious stimulation of the corneal surface can alter nerve morphology and neurochemistry. We used concentrations of menthol, capsaicin, and hypertonic saline that evoked comparable levels of nocifensive eye wipe behaviors when applied to the ocular surface of an awake rat. Animals were sacrificed and corneal nerves were examined using immunocytochemistry and three-dimensional volumetric analyses. We found that menthol and capsaicin both caused a significant reduction in corneal nerve density as detected with β-tubulin immunoreactivity 2 hr after stimulation. Hypertonic saline did not reduce nerve density, but did cause qualitative changes in nerves including enlarged varicosities that were also seen following capsaicin and menthol stimulation. All three types of noxious stimuli caused a depletion of CGRP from corneal nerves, indicating that all modalities of noxious stimuli evoked peptide release. Our findings suggest that studies aimed at understanding the relationship between corneal nerve morphology and chronic disease may also need to consider the effects of acute stimulation on corneal nerve morphology.

KEYWORDS
β-tubulin, CGRP, confocal microscopy, immunocytochemistry, RRID: AB_572217, RRID: AB_2315777, RRID: AB_2492288, RRID: AB_10063408, RRID: SCR_007370, RRID: SCR_013672, RRID: SCR_014199, TRP channels

1 | INTRODUCTION

The cornea is a unique and specialized barrier that protects vulnerable ocular tissues from environmental insults. The cornea is densely innervated with nerves that are tasked with maintaining the integrity of the corneal surface by detecting potentially harmful stimuli and evoking behavioral and reflexive responses to neutralize the stimulus (Shaheen, Bakir, & Jain, 2014). The innervating corneal nerves are primarily nociceptors and these can be classified based on the categories of stimuli that activate the nerve. Corneal nerves can be found that respond selectively to cold stimuli while others respond selectively to mechanical forces, but the majority are classified as polymodal nociceptors that respond to a wide variety of stimuli such as heat, chemical irritants, and inflammatory mediators (Belmonte, Acosta, & Gallar, 2004). The corneal nerves contain receptors that transduce environmental stimuli into nerve activity, including TRPV1 channels that transduce noxious heat stimuli and TRPM8 channels that transduce noxious cold stimuli (Alamri, Bron, Brock, & Ivanusic, 2015; Guo, Vulchanova, Wang, Li, & Elde, 1999; Hiura & Nakagawa, 2012; Ivanusic, Wood, & Brock, 2013; Murata & Masuko, 2006; Nakagawa, Hiura, Mitome, & Ishimura, 2009; Parra et al., 2010). Corneal nerves are also thought to contain osmotic receptors that are sensitive to hypertonic conditions in tears (Chao et al., 2016), although the molecular transducer has not been definitively identified. Polymodal nociceptors are presumed to contain more than one type of these molecular transducers (Chao et al., 2016). Activity from corneal nerves is transmitted via the ophthalmic branch

of the trigeminal nerve to the trigeminal brainstem and supraspinal substrates of nociception, resulting in the perception of ocular pain (Aicher, Hegarty, & Hermes, 2014; Aicher, Hermes, & Hegarty, 2013; Belmonte et al., 2004; Hegarty, Hermes, Largent-Milnes, & Aicher, 2014; Hegarty, Tonsfeldt, Hermes, Helfand, & Aicher, 2010; Marfurt & Del Toro, 1987; Meng & Bereiter, 1996).

Ocular pain can result from corneal exposure to environmental irritants, corneal injuries stemming from accidents, vision correction surgery such as LASIK or general surgery (Altinors, Bozbeyoglu, Karabay, & Akova, 2007; Ang, Dartt, & Tsubota, 2001; Grixti, Sadri, & Watts, 2013). Ocular pain is also seen in chronic conditions such as dry eye disease and normal aging (Chao et al., 2016; Lemp, 2008). Advances in imaging technologies have allowed direct assessment of corneal nerve morphology with the underlying assumption that changes in nerve morphology may be associated with changes in sensory function. For example, in vivo confocal microscopy of corneal nerves is emerging as a clinical assessment tool to measure changes in corneal nerve density and morphology as a means of evaluating neuropathic changes to the corneal nerve population resulting from disorders such as diabetes or dry eye disease (Cruzat, Pavan-Langston, & Hamrah, 2010; Kallinikos et al., 2004). Some studies have observed correlations between nerve morphology and pain states (Altinors et al., 2007; Cruzat et al., 2010; Dworkin, 2002; Theophanous, Jacobs, & Hamrah, 2015; Tuisku, Konttinen, Konttinen, & Tervo, 2008); however, these studies provide conflicting and paradoxical results that make it difficult to establish a direct relationship between corneal nerve integrity and ocular pain.

The effects of chronic disease on corneal nerve morphology may be confounded with changes in nerve morphology induced by acute corneal stimulation. The effect of topical chemical stimulation on the structural integrity of the corneal nerves themselves has only been examined in a few studies (Bates et al., 2010; Harti, Sharkey, & Pierau, 1989; Hirata, Mizerska, Marfurt, & Rosenblatt, 2015). In this study, we quantitatively measured the effects of behaviorally noxious chemical stimuli on the corneal innervation. We developed a method to quantify corneal nerve density and peptidergic content used advanced morphological tools to examine the corneal epithelium in three dimensions.

2 | MATERIALS AND METHODS

2.1 | Experimental animals

All protocols were approved by the Institutional Animal Care and Use Committee at Oregon Health & Science University and all experiments adhered to the guidelines of the National Institutes of Health and the Committee for Research and Ethical Issues of the International Association for the Study of Pain (IASP) for animal experimentation. Male Sprague-Dawley rats (250–400 g; Charles River Laboratories, Wilmington, MA) were housed in pairs on a 12/12 light/dark cycle and were given access to food and water ad libitum. A total of 27 animals were used for all experiments; the specific number of animals used in each study is indicated in the Results section. In some cases, the same animal was used for both behavior study and corneal nerve analysis.

2.2 | Behavioral measurement of ocular sensation

Animals were acclimated to the behavior room and handling for 2 days prior to behavioral assessment. On the day of assessment, awake rats were lightly restrained while 10 μl of a chemical stimulus (menthol, capsaicin, hypertonic saline or vehicle) was applied to the ocular surface (Aicher, Hermes, & Hegarty, 2015). Immediately after application of the stimulus, the animal was placed into a plexiglass chamber and the number of ipsilateral eye wipes made with the corresponding forelimb was counted for 3 min (Aicher et al., 2015; Farazifard, Safarpour, Sheibani, & Javan, 2005; Hegarty et al., 2014). Facial grooming behaviors or hind paw scratches were not counted as eye wipes (Klein, Carstens, & Carstens, 2011; Shimada & LaMotte, 2008). Animals receiving an ocular stimulus were then returned to the home cage for 2 hr until they were sacrificed (see below). A group of animals that received capsaicin was returned to the home cage after behavioral testing and was sacrificed 1 week later. A group of age and weight-matched naïve animals that did not receive any stimulation was included in our corneal studies (see below) to evaluate whether vehicle application had any effect on corneal density in control animals.

2.3 | Ocular stimuli

Prior to the start of the current study, we determined doses of the chemical stimuli that are psychophysically equivalent by eliciting similar numbers of eye wipe responses (Aicher et al., 2015; Farazifard et al., 2005). The osmolalities of the chemicals used for ocular stimulation were measured on a vapor pressure osmometer (VAPRO Model 5600, Wescor, Inc., Logan, UT). Vehicle control animals received 0.9% saline containing 4% ethanol, 4% Tween-80 (Sigma-Aldrich, St. Louis, MO) (295 mOsm). Chemical stimuli for experimental animals included: 50 mM menthol ((Sigma) in 4% ethanol, 4% Tween-80 in 0.9% saline (298 mOsm)); 33 μM capsaicin ((Sigma) in 0.01% ethanol, 0.01% Tween-80 in 0.9% saline (286 mOsm)); and 5 M hypertonic saline (9,430 mOsm).

2.4 | Perfusion and immunocytochemistry

Rats were overdosed with pentobarbital sodium (150 mg/kg) and perfused transcardially as previously described (Hegarty et al., 2014; Hermes, Andresen, & Aicher, 2016) through the ascending aorta with 10 ml heparinized saline (1,000 units/ml) followed by 600 ml 4% paraformaldehyde (in 0.1 M phosphate buffer [PB], pH 7.4). Eyes were enucleated immediately after perfusion and placed in PB. The central cornea was removed from each eye using a 5 mm diameter corneal trephine (Ambler Surgical, Exton, PA) and placed in PB at 4 °C until immunoprocessing. We found that transcardial fixation without post-fixation yielded the best and most consistent labeling of our antigens of interest in corneal afferents.

Whole mount corneas were processed free-floating for immunocytochemistry as previously described (Aicher et al., 2015). Corneas were incubated in a primary antibody cocktail of mouse anti-Neuronal Class III β-tubulin (BioLegend, San Diego, CA) and rabbit anti-calcitonin gene-related peptide (CGRP; ImmunoStar, Hudson, WI) for three nights

TABLE 1 Primary antibodies used for immunocytochemistry

Antibody	Immunogen	Source	Concentration
β-tubulin (clone TUJ1; Neuronal class III)	Rat brain-derived microtubules; C-terminal amino acid sequence (CEAQGPK)	BioLegend Cat# 801201 RRID: AB_10063408 Mouse monoclonal	1:500
CGRP	Full length synthetic rat α-CGRP	ImmunoStar Cat# 24112 RRID: AB_572217 Rabbit polyclonal	1:8,000

at 4 °C. See Table 1 for details on primary antibodies. Corneas were rinsed and incubated in a fluorescent secondary antibody cocktail of Cy3 Donkey anti-Mouse (1:800, Jackson ImmunoResearch Laboratories, Inc., West Grove, PA, Cat# 715-165-151, RRID: AB_2315777) and Alexa Fluor 647 Donkey anti-Rabbit (1:800; Jackson ImmunoResearch, Cat# 711-605-152, RRID: AB_2492288) for 2 hr at room temperature. Corneas were rinsed, blotted dry, and then placed into individual wells of an 18-well μ-Slide (ibidi USA, Inc., Madison, WI) to allow the corneas to maintain their natural convex shape. The slide was coverslipped with CFM-1 (Electron Microscopy Sciences [EMS], Hatfield, PA). A subset of corneas was later clover-leafed, mounted onto slides and coverslipped with Prolong Gold Antifade reagent (Life Technologies, Grand Island, NY) for high magnification analysis.

2.4.1 | Antibody characterization

The primary antibodies used in this study are listed in Table 1 and have been used in previous studies from this laboratory (Aicher et al., 2015; Hegarty et al., 2010). The mouse monoclonal β-tubulin antibody is a well-characterized antibody that was raised against microtubules derived from rat brain (manufacturer's technical specifications). This antibody recognizes an amino acid sequence located in the C-terminus of the neuronal class III β-tubulin protein and produces a single band at 50 kDa on Western blots (Lee, Rebhun, & Frankfurter, 1990; Lischka et al., 2008).

The rabbit polyclonal CGRP antibody was raised against synthetic rat alpha-CGRP (manufacturer's technical specifications). We used this antibody in a previous study to label corneal afferents at their central areas of input into the trigeminal brainstem (Hegarty et al., 2010). The CGRP labeling in corneal nerves in the current study is similar to corneal nerve CGRP labeling in guinea pig (Alamri et al., 2015) and rat (Hiura & Nakagawa, 2012; Jones & Marfurt, 1991, 1998) using other CGRP antibodies. CGRP labeling was completely abolished when this antibody was preadsorbed with the rat alpha-CGRP peptide at a concentration of 10^{-5}, but not other peptides such as substance P (manufacturer's technical specifications) (Hegarty et al., 2010). The specificity of the secondary antibodies has been confirmed by omitting the primary antibodies or incubating primary antibodies with an incorrect secondary antibody.

2.5 | Confocal microscopy and image analysis

2.5.1 | Corneal nerve density

To assess overall corneal nerve density and CGRP content, we used antibodies to β-tubulin and CGRP and images were captured on a Zeiss LSM 510 META confocal microscope with a 20 × 0.75 NA Plan-Apochromat objective (Carl Zeiss MicroImaging, Thornwood, NY). Corneal images were taken from the central cornea and included the whorl-like vortex as an anchor (Figure 1). Z-stacks of 1 μm optical sections bounded by the vertical extent of β-tubulin (Figure 1a,c) and CGRP (Figure 1b,c) immunoreactivity were captured using the single pass, multi-tracking format. Confocal image sizes in the *x* and *y* plane were the same for every image (2048 × 2048 pixels). The image sizes in the *z* plane were different as we had to accommodate the natural curvature of the cornea. Variation in the *z* plane was corrected by isolating the corneal epithelium labeling from the rest of the image (see below).

Cornea nerve density analysis was performed using Imaris 8.0 software (Bitplane USA, Concord, MA, RRID: SCR_007370) on an offline workstation in the Advanced Light Microscopy Core at OHSU by a blinded observer. In the current study, we defined corneal nerve density as the density of the subbasal and intraepithelial corneal nerves taken together. Only the stimulated cornea was evaluated in each animal in these studies. In naïve animals, only one cornea was used for analysis. To correct for variation in the *z* plane of each confocal scan, the corneal epithelium was isolated from the rest of the image using the manual setting of the Surfaces segmentation tool. Specifically, the orientation of the image was rotated such that the *z* plane was vertical (Figure 2a) and the borders of the corneal epithelium were then outlined by the observer using the Draw function at several spots throughout the *z* plane of the image. The corneal epithelium was defined by the β-tubulin-labeled and CGRP-labeled epithelial and subbasal corneal nerves from the anterior surface of the cornea to the epithelial-stromal border (Figures 1 and 2a). Using several tracings throughout the *z* plane, a surface was created (Figure 2b) that served as a region of interest (ROI) for the rest of the analysis. The volume of the corneal epithelium ROI (Figure 2b) was calculated by the software and recorded as the corneal epithelium volume (μm^3). We then used the Mask Channel function to isolate β-tubulin labeling and CGRP labeling within the corneal epithelium ROI for further analysis.

Using the Surfaces segmentation tool, the β-tubulin labeling within the ROI was thresholded (Figure 2c,e) and a volume (μm^3) was calculated. Due to subtle differences in the corneal epithelium volumes (Table 2), the β-tubulin volume (Figure 2c) was calculated as a percentage of the corneal epithelium volume (Figure 2b) for each cornea and expressed as % β-tubulin or the percent of the epithelium that contained β-tubulin-labeled nerves. For the CGRP analysis, we wanted to measure changes in CGRP specifically within corneal nerves. Therefore, the β-tubulin volume (Figure 2c,e) was established as the ROI and the Mask Channel function was used to further determine CGRP labeling

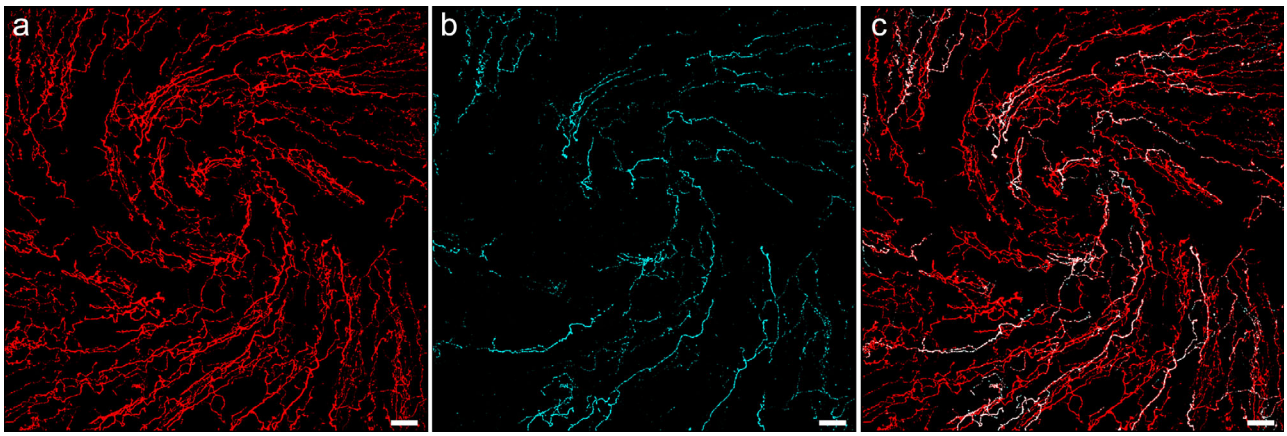

FIGURE 1 Representative confocal images centered over the whorl-like vortex in the central cornea of a naïve rat demonstrate β-tubulin and CGRP-immunolabeled corneal nerves. (a) β-tubulin was used as a marker to visualize all nerves in the rat cornea. (b) CGRP-immunoreactive (-ir) peptidergic nerves are also present in the cornea. (c) The overlay image demonstrates that CGRP-immunoreactive nerves constitute a subset of the entire corneal nerve population. Images are projections of optical slices through the corneal epithelium made using Imaris software. Scale bars = 40 μm [Color figure can be viewed at wileyonlinelibrary.com]

within β-tubulin-labeled nerves. CGRP labeling within nerves was thresholded using the Surfaces segmentation tool (Figure 2d,f) and the volume of CGRP labeling (μm^3) was calculated by Imaris software. As above, the CGRP volume (Figure 2d,f,g) within the β-tubulin ROI (Figure 2c,e,g) of each cornea was normalized to the corneal epithelium volume (Figure 2b) and expressed as % CGRP or the percent of the epithelium that contained CGRP-labeled corneal nerves.

2.5.2 | Varicosity assessment

To assess changes in varicosity morphology, high magnification images were taken from a subset of corneas using a 63 × 1.4 NA Plan-Apochromat oil objective on a Zeiss LSM 780 confocal microscope. These corneas were removed from their wells, clover-leafed, and flat-mounted to achieve proper working distance for the objective. High magnification images of the corneal nerves were captured within the

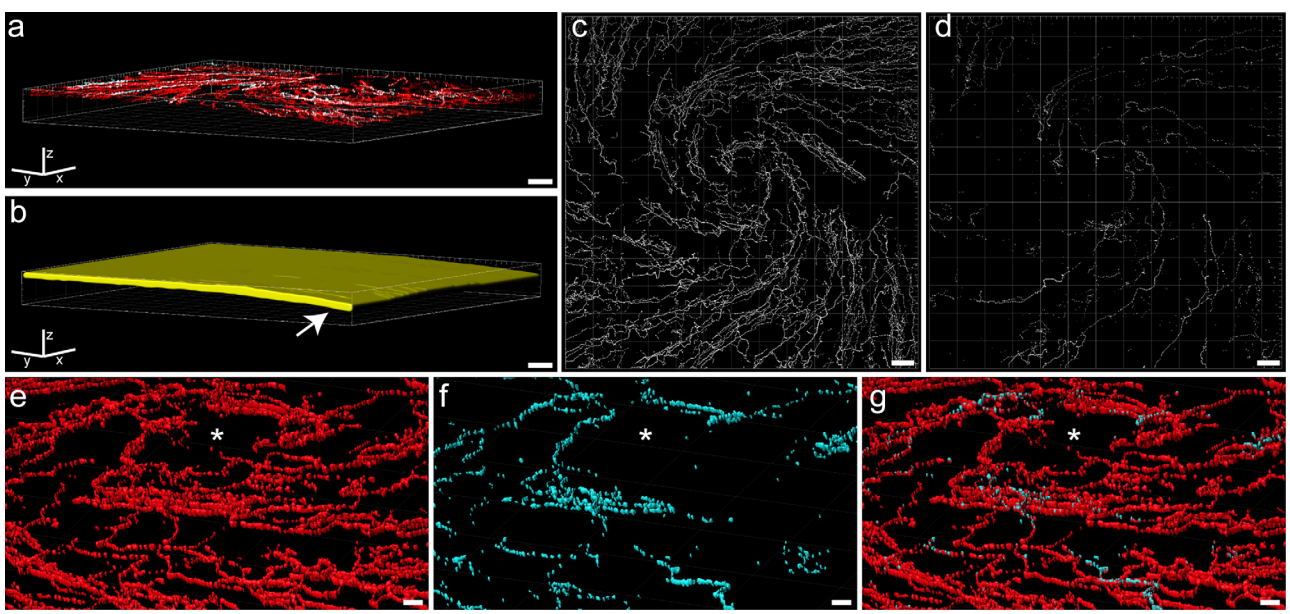

FIGURE 2 Imaris software was used to quantitate nociceptive corneal nerves within the corneal epithelium. All images include the Imaris frame for orientation. (a) The confocal image of the rat cornea from Figure 1c was rotated in Imaris software such that the *z* plane was oriented vertically. The epithelial area was defined by the extent of corneal nerve labeling and was traced at several levels throughout the *z* plane. (b) Imaris then used those tracings to build a region of interest (ROI; yellow area) that included labeling throughout the epithelium. Note the natural curvature of the cornea on the right side (arrow). (c) The volume of β-tubulin labeling was determined within the corneal epithelium ROI. This β-tubulin volume was then used as an ROI to mask the CGRP labeling within β-tubulin-labeled nerves. (d) The volume of CGRP labeling within β-tubulin nerves can be revealed and quantified. By changing the perspective angle, more details can be visualized of the Imaris-calculated β-tubulin (e) and CGRP (f) volumes around the whorl-like vortex (asterisk) within the corneal epithelium. The overlay (g) of these volumes demonstrates populations of corneal nerves with and without CGRP. Scale bars: a–d = 40 μm; e–g = 10 μm. [Color figure can be viewed at wileyonlinelibrary.com]

TABLE 2 Corneal epithelium volumes

Treatment group	Epithelium volume ($\times 10^6$ μm^3)	N
Control	6.8 ± 0.6	7
Menthol	8.2 ± 0.7	4
Capsaicin	5.5 ± 1.1	4
Hypertonic saline	7.0 ± 0.5	4
Long-term capsaicin	7.6 ± 1.4	3

Data expressed as mean ± *SEM*. All volumes have an exponent of $\times 10^6$.

whorl and in a region outside the whorl but within the central cornea. Confocal micrographs used for publication were adjusted for optimal brightness and contrast using Adobe Photoshop CS5 (Adobe Systems Incorporated, San Jose, CA, RRID: SCR_014199).

We noticed that corneal nerve varicosity size appeared to differ among stimulated corneas, so we used high magnification images to qualitatively assess stimulus-induced alterations to the structure of the corneal nerves using Zeiss Zen 2011 (black edition, RRID: SCR_013672) software. Varicosities were operationally defined as punctate enlargements along or at the end of a corneal nerve that were present in two consecutive optical slices (Aicher et al., 2013, 2014; Hegarty et al., 2010, 2014). Two regions were captured per cornea and varicosities were arbitrarily sampled throughout each scanned image. The maximum of the minimum cross-sectional diameter of each varicosity was measured by an observer blinded to experimental condition (25 varicosities per image, 50 varicosities per cornea). The frequency of varicosity diameters from all corneas was displayed using a histogram fitted with a Gaussian peak curve (SigmaPlot 12.0 (Systat Software, Inc., San Jose, CA, RRID: SCR_003210).

2.6 | Statistical analyses

Statistical analyses and curve fitting were performed using SigmaPlot 12.0 software. A one-way ANOVA was performed to test for differences among treatment groups in eye wipe behavioral responses and corneal epithelium volumes. The Holm-Sidak post hoc test was utilized when analyzing the eye wipe responses. A Mann-Whitney Rank Sum test and *t* test were used to compare the % β-tubulin and % CGRP in Naïve and Vehicle corneas, respectively, to pool them as one Control group for further analysis. *T* tests were then used to compare each chemically-stimulated treatment group to Control. In all cases, a *p* value less than 0.05 was considered significant.

3 | RESULTS

3.1 | Different ocular chemical stimuli evoke similar eye wipe responses

The purpose of this study is to determine if noxious ocular stimulation alters the morphology and neurochemistry of corneal sensory nerves (Figure 1). Application of noxious chemical stimuli to the corneal surface of awake rats evoked stereotypical forelimb eye wipe behavior (Figure 3a). We selected doses of menthol, capsaicin, and hypertonic saline that elicited similar numbers of eye wipes (Figure 3a). As a control, we used the vehicle solution used to prepare the menthol stimulus. We found that eye wipes evoked by ocular application of 50 mM menthol, 33 μM capsaicin, and 5 M hypertonic saline were all significantly different from vehicle, but were not different from each other (one way ANOVA ($p < 0.001$), Holm-Sidak post hoc tests, $p \leq 0.001$ for all stimuli as compared to Vehicle) (Figure 3a). These results demonstrate that among this diverse set of chemical stimuli, we have achieved behaviorally equivalent doses for corneal nociception.

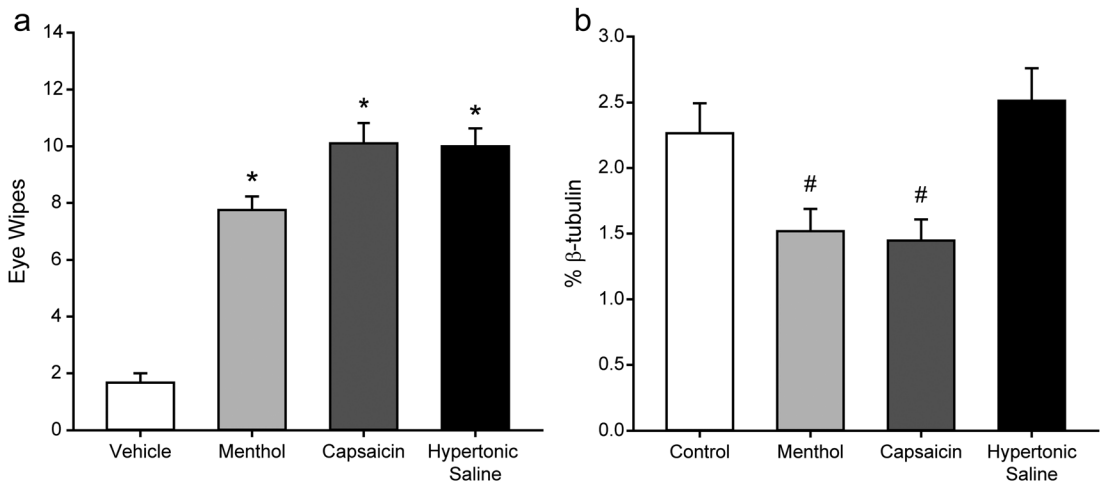

FIGURE 3 Stimuli of different modalities induce similar eye wipe responses in rats but produce differential effects on the corneal nerves. (a) Application of menthol (50 mM, $n = 4$), capsaicin (33 μM, $n = 10$), or hypertonic saline (5 M, $n = 5$) to the ocular surface induce significant numbers of ipsilateral eye wipes compared to vehicle ($n = 3$). (b) β-tubulin immunolabeling in the corneal epithelium is reduced after ocular application of menthol ($n = 4$) or capsaicin ($n = 4$) as compared to Control corneas ($n = 7$). In contrast, hypertonic saline did not alter corneal β-tubulin immunolabeling ($n = 4$). Bars indicate mean ± *SEM*. *$p < 0.05$ versus Vehicle; #$p < 0.05$ versus Control.

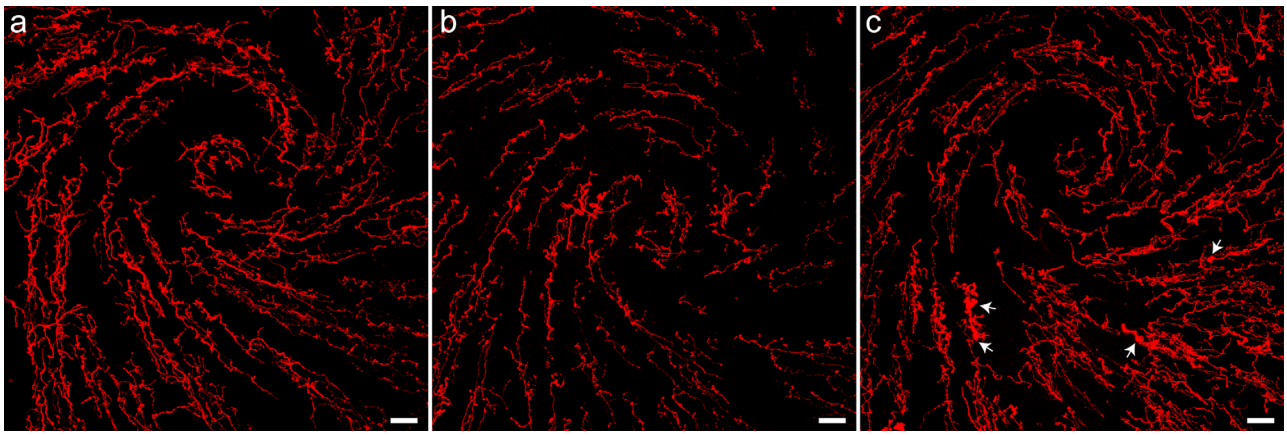

FIGURE 4 Representative images of the β-tubulin labeling demonstrate the acute and long-term effects of capsaicin stimulation of the cornea. (a) β-tubulin labeling around the whorl-like vortex in the central cornea of a Control animal that received vehicle solution. (b) β-tubulin is markedly decreased 2 hr after capsaicin stimulation. (c) Nerve density is increased 1 week after capsaicin, but abnormal varicosities are still apparent (arrows). Images are projections of optical slices taken through the corneal epithelium made using Imaris software. Scale bars = 40 μm [Color figure can be viewed at wileyonlinelibrary.com]

3.2 | Corneal epithelium volume is not affected by chemical stimulation

We used immunocytochemistry to identify corneal nerves and their content of CGRP (Figure 1). For quantification, we limited our analyses to corneal nerves within a defined volume of the corneal epithelium (Figure 2a,b). To ensure the corneal epithelial volume was similar between groups we compared two groups of control corneas: corneas that received application of the vehicle control solution (Vehicle) and corneas that received no stimulation (Naïve). The volume of the corneal epithelium was not significantly different between these two groups (All volumes have an exponent of $\times 10^6$; Vehicle: $6.1 \pm 0.2\,\mu m^3$, $n = 3$; Naïve: $7.3 \pm 1.0\,\mu m^3$, $n = 4$; t test, $p = 0.192$). Therefore, these two groups of corneas were pooled as the Control group for further analysis. Corneal epithelium volumes are listed in Table 2 for all treatment groups in this study. We compared all acutely stimulated corneas (Menthol, Capsaicin, Hypertonic Saline) and a group of corneas that were stimulated and then perfused 1 week later (Long-term Capsaicin). There were no significant differences in corneal epithelial volume between any of these groups (one-way ANOVA, $p = 0.242$).

3.3 | Corneal β-tubulin labeling is reduced after application of menthol or capsaicin

Corneal nerves contain β-tubulin and assessment of this marker is often used as an index of nerve density (Aicher et al., 2015; Dvorscak & Marfurt, 2008; Hirata et al., 2015). We tested the hypothesis that noxious stimulation of the cornea can alter corneal nerve density. To conduct a three dimensional analysis, we normalized the volume of β-tubulin labeling to the corneal epithelium volume (% β-tubulin) for each cornea to account for any individual differences in epithelial volume among all of the corneas tested (Figure 2). We first assessed % β-tubulin in Vehicle ($2.1 \pm 0.5\%$, $n = 3$) and Naïve ($2.4 \pm 0.2\%$, $n = 4$) corneas and found no significant differences between these groups (Mann-Whitney Rank Sum test, $p = 0.857$). Therefore, the Vehicle and Naïve groups were pooled as the Control group for further analysis. The % β-tubulin values were then compared between Control corneas and individual groups of acutely stimulated corneas. A single application of menthol caused a significant reduction in % β-tubulin when compared to Control corneas (Figure 3b; t test, $p = 0.026$, $n = 7$ Control, 4 Menthol). An acute, single application of capsaicin also significantly reduced the % β-tubulin in treated corneas as compared to Control (Figure 3b; t test, $p = 0.018$, $n = 7$ Control, 4 Capsaicin). This is in contrast to a single application of hypertonic saline which did not change % β-tubulin (Figure 3b; t test, $p = 0.253$, $n = 7$ Control, 4 Hypertonic Saline). These results demonstrate that even a single application of menthol or capsaicin can reduce corneal nerve density 2 hr later. Although all three stimuli (menthol, capsaicin, and hypertonic saline) elicited psychophysically equivalent behavioral responses (Figure 3a), only the menthol and capsaicin reduced corneal nerve density (Figure 3b).

To determine whether corneal nerves show long-term changes after a single capsaicin stimulation, a subset of animals that received corneal application of capsaicin were examined 1 week later. When qualitatively compared to a Control cornea (Figure 4a) and an acutely stimulated Capsaicin cornea (Figure 4b), the nerves in the cornea that received capsaicin stimulation 1 week prior (Long-term Capsaicin) contained some irregular nerve morphology (Figure 4c, arrows) and a somewhat lower nerve density. The % β-tubulin values in the Long-term Capsaicin corneas ($1.8 \pm 0.2\%$, $n = 3$) are intermediate between the % β-tubulin values from Control ($2.3 \pm 0.2\%$, $n = 7$) and acute Capsaicin ($1.4 \pm 0.2\%$, $n = 4$) corneas. These results suggest that the corneal nerves undergo persistent dynamic changes in response to a single ocular chemical stimulus that are still evident 1 week later.

3.4 | CGRP is depleted from corneal nerves by different noxious stimuli

We examined the CGRP content of corneal nerves to determine whether ocular chemical stimuli specifically affected CGRP-containing

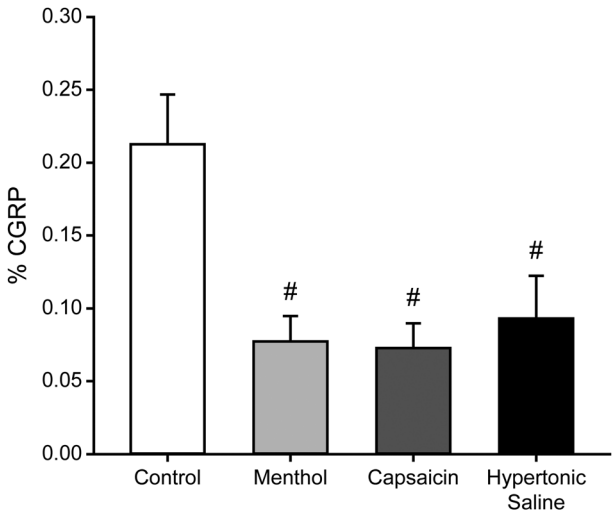

FIGURE 5 CGRP is reduced after acute noxious corneal stimulation. CGRP immunolabeling within epithelial corneal nerves is reduced after ocular application of menthol ($n = 4$), capsaicin ($n = 4$) or hypertonic saline ($n = 4$) as compared to Control corneas ($n = 7$). Bars indicate mean ± *SEM*. #$p < 0.05$ versus Control.

nerves. The volume of epithelial CGRP labeling was measured within the mask created by the β-tubulin labeling present in each cornea (Figure 2) to obtain the percent of nerve volume containing CGRP. There were no significant differences in % CGRP between Vehicle and Naïve corneas (Vehicle: 0.24 ± 0.07%, $n = 4$; Naïve: 0.19 ± 0.04%, $n = 3$; *t* test, $p = 0.271$). Therefore, these two groups were pooled as the Control group. The % CGRP values were compared between Control corneas and each group of acutely chemically stimulated corneas. When compared to Control corneas ($n = 7$), Menthol (*t* test, $p = 0.01$, $n = 4$), Capsaicin (*t* test, $p = 0.009$, $n = 4$), and Hypertonic Saline (*t* test, $p = 0.022$, $n = 4$) corneas all showed significantly reduced % CGRP after an acute, single ocular application (Figure 5). This suggests that CGRP is depleted by stimuli that are noxious enough to elicit nociceptive behavioral eye wipe responses (Figure 3a), regardless of whether nerve density is reduced (Figure 3b).

A similar analysis was conducted on a group of rats exposed to capsaicin 1 week prior (Long-term Capsaicin treatment). Similar to % β-tubulin, the % CGRP values from Long-term Capsaicin corneas (0.12 ± 0.03%, $n = 3$) were intermediate between % CGRP values from Control (Figure 5; 0.21 ± 0.03%, $n = 7$) and Capsaicin (Figure 5; 0.07 ± 0.02%, $n = 4$) corneas. This suggests that the effects of capsaicin stimulation persist in CGRP-containing corneal nerves.

3.5 | Corneal nerve varicosities are acutely affected by noxious ocular stimuli

High magnification images of central corneal nerves were qualitatively assessed for stimulus-induced changes in nerve structure (Figure 6). We noted that the varicosities dotting the intraepithelial corneal nerves appeared to be distended in some cases. We assessed this by measuring the cross-sectional diameter of 50 representative varicosities in one cornea per treatment group. In the images taken from a Control cornea, all varicosities on corneal nerves fell within the range of 0.4 to 1.5 μm in diameter (Figure 6a; white bars). The majority of varicosities from stimulated animals were 1.5 μm or smaller, but stimulated corneas also had a few very large varicosities (Figure 6a; gray striped bars). Corneal nerves from a Control animal appeared normal with thin nerves beaded with small varicosities (Figure 6b). In contrast, corneas exposed to noxious chemical stimuli, including cases for Long-term Capsaicin treatment 1 week prior (Figure 4c), contained varicosities that appeared distended and measured greater than 1.5 μm in diameter. Although hypertonic saline did not affect the overall corneal % β-tubulin density (Figure 3b), it did induce enlarged varicosities (Figure 6c) 2 hr after application.

4 | DISCUSSION

We have demonstrated that corneal nerves are differentially affected by psychophysically equivalent doses of noxious chemical stimuli applied to the corneal surface. We have combined behavioral assessments of corneal nociception with quantitative imaging tools and qualitative observations to assess the effects of noxious chemical stimulation on corneal nerves. Eye wipe responses to noxious stimuli were used to establish doses of chemical stimuli and are in agreement with previous studies from this laboratory (Aicher et al., 2015; Hegarty et al., 2014) and others (Farazifard et al., 2005). We used β-tubulin, a well-characterized nerve marker to study the overall changes in corneal nerve density in the central area of the cornea (Aicher et al., 2015; Dvorscak & Marfurt, 2008; Hirata et al., 2015), while CGRP was also used to address whether subgroups of nociceptive nerves were specifically affected by select noxious ocular stimuli (Belmonte et al., 2004; Hegarty et al., 2010). We found that the density of β-tubulin-labeled corneal nerves within the epithelium was significantly reduced by capsaicin and menthol, but not by hypertonic saline. Stimulus-induced CGRP depletion from corneal nerves was caused by all of the noxious stimuli tested. This study underscores that even a single application of a noxious stimulus produces acute morphological and neurochemical changes in the corneal nerve population. This study also suggests that a single application of a noxious stimulus may have long-lasting effects on these vulnerable peripheral nerves.

4.1 | Methodological considerations

We developed a protocol combining well-established immunocytochemical methods and confocal microscopy with advanced imaging tools for assessing corneal nerve density and neurochemical composition (see Methods). This approach improves upon our previous work in the cornea (Aicher et al., 2015) by allowing widefield, high resolution imaging. By mounting the corneas in individual wells, we are able to maintain the natural curvature of the cornea and avoid the need to clover-leaf and flat-mount them on to slides. By using advanced imaging tools, we are able to compensate for variations in z-thickness and orientation and thereby limit our analyses specifically to the corneal epithelium. We found that there were some subtle differences in epithelium volume among individual corneas that may be due to variations

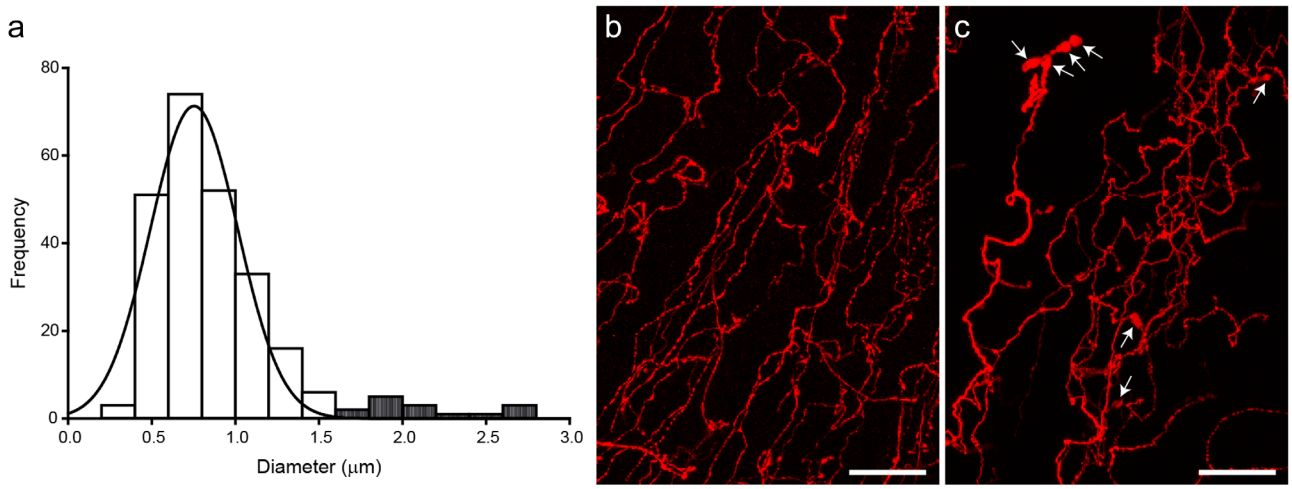

FIGURE 6 Corneal nerve varicosities are enlarged after acute noxious chemical stimulation. (a) A histogram displaying the frequency of cross-sectional diameters measured from 250 varicosities (25 varicosities/scan, 2 scans/cornea, 1 cornea/animal; $n = 5$ animals) and fitted with a peak Gaussian curve. White bars represent the varicosity diameters measured from a Control cornea and the majority of varicosities from stimulated corneas. Striped bars represent those large varicosities only found in stimulated corneas. (b) High magnification image of β-tubulin-labeled corneal nerves from a Naïve animal demonstrates thin nerves beaded with varicosities. (c) Hypertonic saline stimulation leads to distended varicosities (arrows). Images are projections of optical slices taken through the corneal epithelium. Scale bars = 20 μm [Color figure can be viewed at wileyonlinelibrary.com]

in z-thickness, natural differences among animals, and variations in the experimenter tracing the outline of the corneal epithelium. Despite these sources of variation, we did not find any significant differences in corneal epithelium volume among any of the treatment groups (Table 2). We calculated volumes for each marker as a portion of the epithelium volume for each cornea to allow between animal comparisons. Therefore, the differences we found in % β-tubulin (Figure 3b) are not attributable to differences in epithelium volume.

We also used the advanced imaging approach to quantify CGRP loss from corneal nerves. Over the course of our studies, we found that CGRP labeling in the cornea was not always limited to nerves. We occasionally observed extra-nerve fiber labeling within the corneal epithelium that we speculate could be background labeling or may represent CGRP that has been released from nerves into the epithelial space by noxious stimuli. Therefore, to assess CGRP content specifically within corneal nerves, we isolated the CGRP labeling within an ROI created from the volume of epithelial β-tubulin labeling (Figure 2c) and created a new volume representing CGRP labeling within the corneal nerves (Figure 2d). By limiting CGRP volume measurements to the β-tubulin ROI within the epithelium volume ROI, we make our best approximation of changes in CGRP within corneal nerves, even after stimulus-induced nerve loss.

4.2 | CGRP content of corneal nerves is reduced by all noxious stimuli tested

We demonstrate that CGRP is reduced by all the noxious stimuli we applied to the cornea, suggesting that CGRP-containing nerves are vulnerable to different types of noxious insults, not just the TRPV1-specific agonist capsaicin. If CGRP-immunoreactive nerves were selectively responsive to capsaicin stimulation, we would have expected a more profound loss of CGRP compared to menthol stimulation or hypertonic saline. Both capsaicin and menthol caused a reduction in overall β-tubulin density, so the assessment of CGRP depletion is more complex in these cases. However, we conducted our analysis in a manner that compared the CGRP within the remaining nerve content as a percent of the corneal epithelium volume, so that we might detect differences even in the face of changes in overall nerve density. For both Menthol and Capsaicin corneas, it is possible that the CGRP reduction is due to loss or disruption of those nerves. However, we also saw a reduction in CGRP immunoreactivity for cases treated with hypertonic saline. Since the Hypertonic Saline corneas did not show a change in β-tubulin density, our data suggest that all of these stimuli are sufficient to induce the release of CGRP from corneal sensory nerves. CGRP is thought to contribute to the sensitization of local nociceptors as well as promote the integrity and health of epithelial tissues (Alamri et al., 2015; Muller, Marfurt, Kruse, & Tervo, 2003). CGRP has been shown to promote wound healing of bronchial epithelial cells (Zhou et al., 2013), induce the synthesis of the neutrophil-recruiting chemokine IL-8 within corneal epithelial cells (Tran, Ritchie, Lausch, & Oakes, 2000) and promote the stratification of corneal epithelial cells (Ko et al., 2014). Therefore, chronic depletion of CGRP could compromise the integrity of the corneal epithelium.

4.3 | Capsaicin stimulation alters corneal nerve morphology and neurochemistry

Capsaicin is an agonist of the transient receptor potential vanilloid 1 (TRPV1) channel, a cationic channel that is permeable to calcium and sodium (Caterina et al., 1997, 2000; Patapoutian, Tate, & Woolf, 2009).

Several studies have demonstrated that capsaicin and the more potent TRPV1 agonist resiniferatoxin (RTX) are noxious stimuli to orofacial structures in rodents (Aicher et al., 2015; Caterina et al., 2000; Hegarty et al., 2014; Klein et al., 2011; Neubert et al., 2008; Shimada & LaMotte, 2008). These agonists have been also shown to have cytotoxic effects on neurons in culture (Goswami, Dreger, Otto, Schwappach, & Hucho, 2006; Han et al., 2007). Previous studies have demonstrated loss of the corneal nerves in adulthood after systemic injection of TRPV1 agonists into neonates (Fujita, Miyazono, & Ohba, 1987; Lambiase et al., 2012; Marfurt, Ellis, & Jones, 1993; Ogilvy & Borges, 1990). Other studies have looked at the effects of topical capsaicin or RTX on corneal nerves and have found that CGRP-labeled nerves were lost after application of a TRPV1 agonist. One study in rats found a 50% reduction in the number of CGRP- and substance P (SP)-labeled nerves after repeated topical applications of a high concentration of capsaicin over the course of 5 days (Harti et al., 1989). A more recent study used topical application of RTX to the rat cornea to look at changes to β-tubulin and CGRP-labeled corneal nerves, but due to methodological constraints, only assessed changes in stromal nerve bundles (Bates et al., 2010). This study demonstrated a reduction in CGRP-labeled nerves within β-tubulin-labeled stromal nerve bundles that they attributed to ablation of CGRP-labeled nerves or depletion of CGRP (Bates et al., 2010). In our current study, we used advanced imaging techniques to examine the entire depth of the corneal epithelium, including intraepithelial and subbasal corneal nerves. Our study demonstrates a loss of corneal nerves as well as a reduction in CGRP content in the remaining nerves after a single application of capsaicin. We find that these effects are sustained at 2 hr after stimulation and morphological changes are still evident 1 week later.

The influx of calcium through the TRPV1 channels may lead to changes in sensory nerve morphology by different mechanisms which could lead to reversible peripheral nerve injury or irreversible cell death, depending on the site of activation (Patapoutian et al., 2009). Of special relevance to the current study, one potential mechanism underlying TRPV1-induced cytotoxicity involves the effects of TRPV1 activation on the neuronal microtubule cytoskeleton. Microtubules provide neurons with structure and guide transport of proteins and organelles to all parts of the neuron. The dynamic nature of microtubule assembly and disassembly is critical to axon growth during development and regrowth after injury (Kapitein & Hoogenraad, 2015). RTX-induced TRPV1 activation within cultured DRG cells led to the dispersal of the tubulin cytoskeleton within 1 min of application (Goswami et al., 2006). This study goes on to suggest that calcium influx via activated TRPV1 channels contributes to the depolymerization of microtubules, leading to a disruption of the cytoskeleton which could potentially induce cellular degeneration (Goswami et al., 2006). In another study, capsaicin activation of TRPV1 was found to induce rapid calcium influx into cultured cells that was sustained for at least 20 min. This increase in intracellular calcium increased cell body size, rapidly depolymerized microtubules within 10 min of capsaicin application and led to shrinkage of cellular processes in a subset of cells (Han et al., 2007). The loss of β-tubulin in our study suggests that the TRPV1 agonist can also disrupt axonal microtubules in vivo, even after a brief application to the cornea. We could not determine whether the affected nerves had been removed from the corneal epithelium or distorted beyond our ability to image them. It is possible that the loss of β-tubulin labeling may reflect the thinning of the corneal nerves beyond what can be resolved by the confocal microscope. Regardless, our results point to neuropathic changes in the corneal nerves after a single application of certain noxious stimuli.

4.4 | Menthol stimulation alters corneal nerve morphology and neurochemistry

Menthol is an agonist of the TRPM8 channel which is the primary molecular transducer involved in transmission of noxious cold stimulation (Bautista et al., 2007; McKemy, Neuhausser, & Julius, 2002). In the cornea, TRPM8-containing sensory nerves are involved in mediating responses to ocular application of menthol and are thought to be important for tear production, thus providing an important mechanism for sustaining the protective environment on the corneal surface (Acosta, Belmonte, & Gallar, 2001; Madrid et al., 2006; Parra et al., 2010; Robbins, Kurose, Winterson, & Meng, 2012). In the current study, we used a dose of menthol sufficient to elicit nociceptive eye wipe responses similar to those seen with capsaicin in rats (Aicher et al., 2015) because we wanted to compare equally noxious stimuli. Surprisingly, we find that a noxious dose of menthol is able to disrupt corneal nerves in a similar manner and to a similar extent as capsaicin. Menthol stimulation produced a significant loss of corneal nerve labeling with β-tubulin and also caused the depletion of CGRP from remaining corneal nerves. To our knowledge, this is the first study to examine the acute effects of noxious menthol on the structural integrity of corneal nerves.

The similarities between menthol- and capsaicin-stimulated corneas suggest that TRP agonists may share a common mechanism that leads to the disruption of corneal nerve morphology. One of the unifying features of TRP agonist-induced neuronal activation is the influx of calcium (Almaraz, Manenschijn, de la Pena, & Viana, 2014; McKemy et al., 2002; Patapoutian et al., 2009). Unlike the TRPV1 agonists, examination of the cytotoxic effects of menthol has primarily been limited to in vitro studies in cancer cell lines. Menthol-induced cytotoxicity and reductions in cancer cell numbers have been demonstrated in A-375 malignant melanoma (Kijpornyongpan, Sereemaspun, & Chanchao, 2014), Caco-2 human epithelial colorectal adenocarcinoma (Faridi et al., 2011), human bladder cancer T24 (Li, Wang, Yang, Wang, & Li, 2009), human leukemia HL-60 (Lu et al., 2006) and murine WEHI-3 leukemia (Lu et al., 2007) cells. Some of these studies found menthol-induced increases in calcium influx into these cancer cells, suggesting that calcium influx led to cell death (Kijpornyongpan et al., 2014; Lu et al., 2006). Another study found menthol-induced reductions in tubulin proteins, modulation of tubulin polymerization and ultimately an increase in apoptosis of Caco-2 epithelial colorectal adenocarcinoma cells, suggesting a novel mechanism of menthol-induced cell death involving microtubule integrity (Faridi et al., 2011).

Topical menthol application evokes a cold sensation that is accompanied by discomfort and a painful burning sensation in humans (Acosta et al., 2001; Wasner, Schattschneider, Binder, & Baron, 2004).

Studies have demonstrated the co-expression of TRPM8 and TRPV1 in populations of small diameter dorsal root ganglia (DRG) and trigeminal ganglia (TG) neurons (Alamri et al., 2015; McKemy et al., 2002; Takashima et al., 2007; Xing, Ling, Chen, & Gu, 2006), suggesting that the sensation of pain evoked from noxious menthol is due to activation of polymodal nociceptors that express TRPV1 (McKemy et al., 2002; Wasner et al., 2004; Xing et al., 2006). Previous studies have also demonstrated the co-expression of TRPM8 and the nociceptive peptide CGRP in trigeminal neurons (Abe et al., 2005; Takashima et al., 2007). Our results support the notion that noxious doses of menthol likely activate polymodal nociceptors, leading to behavioral responses and changes to corneal nerve morphology equivalent to that seen in capsaicin-stimulated animals.

Doses of menthol similar to the ones used in the current study, have also been shown to evoke eye wipe responses (Robbins et al., 2012) and trigger expression of a nerve injury marker (Braz & Basbaum, 2010) in TRPM8 knockout mice, suggesting a TRPM8-independent activation of nociceptive neurons. It is possible that noxious doses of menthol may be capable of directly activating receptors in addition to TRPM8. It is thought that only 10–15% of corneal nerves are cold-sensitive (Belmonte et al., 2004), however the results of the current study would suggest that more corneal nerves than that were affected by noxious menthol. This is consistent with the notion that other nociceptors, such as polymodal nociceptors, may also be responsive to noxious doses of menthol. A recent review suggested that a variety of other TRP, potassium and sodium channels may be involved in the transduction or modulation of cold pain from peripheral afferents (Lolignier et al., 2016). However, it is unclear if any of these channels could be directly activated by menthol in the absence of TRPM8. Thus, the menthol-induced effect on corneal afferents may be similar to those of capsaicin because the intensity of the stimulation is also activating non-TRPM8 receptors, because both channels are localized on corneal polymodal nociceptors, or because each stimulus elicits similar downstream cytotoxic mechanisms following calcium influx.

4.5 | Hypertonic saline stimulation alters corneal nerve neurochemistry

We have demonstrated that hypertonic saline is a noxious stimulus to the cornea, which is in agreement with previous studies in rats (Farazifard et al., 2005) and humans (Liu et al., 2009). Similar to capsaicin and menthol, a single stimulation with noxious intensity hypertonic saline significantly depleted CGRP from corneal nerves. In contrast to the TRP channel agonists, hypertonic saline did not cause a reduction in corneal nerve density. These results suggest that activation of nociceptors alone is not sufficient to disrupt β-tubulin in sensory axons and alter nerve density. This could be because hypertonic saline is activating a different population of nociceptors or because it is activating different intracellular mechanisms in nociceptors.

The identification of a specific corneal osmoreceptor has been elusive, although many studies have looked at the effect of hyperosmolar solutions in the context of reflex tearing and dry eye disease. A recent study demonstrated an increase in activation of cold-sensitive trigeminal ganglion neurons after brief corneal stimulation with supraphysiological hyperosmolar solutions (Hirata & Meng, 2010). Other studies have shown that longer stimulation of corneal nerve terminals with supraphysiological hyperosmolar solutions altered corneal nerve terminal firing patterns of both cold thermoceptor and polymodal nociceptors (Parra, Gonzalez-Gonzalez, Gallar, & Belmonte, 2014) and led to the disappearance of responses of both low- and high-threshold cold-sensitive corneal neurons to corneal drying (Hirata et al., 2015). Last, in vitro and in vivo studies using TRPM8 knockout mice demonstrated that the TRPM8 channel is an osmosensor in detecting increases in osmolality (Quallo et al., 2015). Therefore, TRPM8-containing cold thermoceptors in the cornea may act as sensors for fluctuations in physiologically relevant levels of osmolality, but supraphysiological hyperosmolar solutions may recruit polymodal nociceptors to transduce this noxious stimulus (Hirata et al., 2015; Liu et al., 2009; Parra et al., 2014; Quallo et al., 2015). The specific channels that transduce noxious hyperosmolar stimulation are unknown, although studies on centrally-regulated systemic osmoregulation have implicated a variant of the TRPV1 channel as an osmosensor (Zaelzer et al., 2015).

Since the majority of the corneal nerves are polymodal, it is likely that stimulation with hypertonic saline activates the same nociceptors but engages a different set of downstream signaling and effector systems than was activated with the TRP agonists. While overall nerve density was not altered, we did see morphological changes in corneal nerves after hypertonic saline, including increases in the size of varicosities. This finding is similar to morphological changes reported by others following sustained application of hypertonic saline to the rodent eye in an anesthetized preparation (Hirata et al., 2015). In those studies, the stimulus was left on the eye for a much longer duration, so our study is important in showing that even a brief application of this noxious stimulus, which is wiped away by the rat in less than 1 min is sufficient to both release CGRP and also induce changes in nerve varicosities.

While we do not know the underlying mechanisms, a study modeling traumatic brain injury in isolated axon cultures found that rapid mechanical stretching of axons results in enlarged focal axon swellings within 3 hr and eventual degeneration after 24 hr of injury (Tang-Schomer, Patel, Baas, & Smith, 2010). This study demonstrated that the microtubules within the focal swellings had ruptured and became disorganized, likely disrupting axonal transport, which would lead to the accumulation of protein, an increase in swelling and eventual degeneration (Tang-Schomer et al., 2010). Therefore, one possibility in our study is that the hypertonic saline acts as a profound osmotic stimulus that causes axon swelling mimicking mechanical stretch. Studies of central nociceptor nerves have shown that stimulation with intense heat or substance P can evoke changes in nerve morphology that includes enlarged varicosities and thinning of adjacent nerves which is thought to be due to internalization of the substance P receptor; these changes reverse in less than 1 hr after termination of the stimulus (Mantyh et al., 1995).

4.6 | Functional implications and conclusions

In our studies, we find that noxious chemical stimulation of the cornea produced changes in corneal nerve morphology that may alter interpretation

of imaging studies and may also alter nerve function. Humans with ocular exposure to pepper spray have been shown to have changes in sensation (Vesaluoma et al., 2000), with modality-specific decreases in sensation for several days following exposure, consistent with our findings of a reduction in nerve density. Also, menthol is used in some eye drop formulations to reduce ocular pain (Kurose & Meng, 2013). Our data suggest that both chemicals may alter sensory function by temporarily disrupting nerve morphology. Noxious doses of capsaicin and menthol injected into the rodent hind paw have been shown to increase the expression of a nerve injury marker, activating transcription factor 3 (ATF3), in DRG neurons (Braz & Basbaum, 2010) supporting the notion that these TRP agonists can impact nerve health. Together these findings show that a single noxious stimulus applied to the ocular surface can alter nerve morphology for hours and in some cases even for days. Studies from other groups indicate that application of capsaicin or menthol can reduce sensitivity, although responses may depend on intensity and duration of the chemical stimulus and time between stimulation and testing (Almaraz et al., 2014; Belmonte, Gallar, Pozo, & Rebollo, 1991; Carstens, Kuenzler, & Handwerker, 1998; Caterina & Julius, 2001; Cliff & Green, 1994; McKemy et al., 2002; Szolcsanyi, Jancso-Gabor, & Joo, 1975). Our results indicate that viewing changes in nerve density as an index of chronic disease may be confounded by neural responses to acute stimulation. Thus, a complete history may be important in aiding the interpretation of corneal nerve morphology in patients.

ACKNOWLEDGMENTS

The authors wish to thank Dr. Stefanie Kaech Petrie and Aurelie Snyder of the OHSU Advanced Light Microscopy Imaging Core for their guidance on the preparation, imaging, and analysis of the corneas used in this study.

CONFLICT OF INTEREST

The authors do not have any conflicts of interest.

AUTHOR CONTRIBUTION

All authors had full access to all the data in the study and take responsibility for the integrity of the data and the accuracy of the data analysis. Study concept and design: SAA, DMH, SMH. Acquisition of data: DMH, SMH, KY. Analysis and interpretation of data: DMH, SMH, SAA. Drafting of the manuscript: DMH, SAA. Critical revision of the manuscript for important intellectual content: DMH, SMH, SAA. Statistical analysis: DMH, SAA. Obtained funding: SAA. Administrative, technical and material support: DMH, SMH, KY, SAA. Study supervision: SAA.

DATA ACCESSIBILITY

n/a

REFERENCES

Abe, J., Hosokawa, H., Okazawa, M., Kandachi, M., Sawada, Y., Yamanaka, K., … Kobayashi, S. (2005). TRPM8 protein localization in trigeminal ganglion and taste papillae. *Brain Research. Molecular Brain Research*, *136*(1–2), 91–98.

Acosta, M. C., Belmonte, C., & Gallar, J. (2001). Sensory experiences in humans and single-unit activity in cats evoked by polymodal stimulation of the cornea. *The Journal of Physiology*, *534*(Pt. 2), 511–525.

Aicher, S. A., Hegarty, D. M., & Hermes, S. M. (2014). Corneal pain activates a trigemino-parabrachial pathway in rats. *Brain Research*, *1550*, 18–26.

Aicher, S. A., Hermes, S. M., & Hegarty, D. M. (2013). Corneal afferents differentially target thalamic- and parabrachial-projecting neurons in spinal trigeminal nucleus caudalis. *Neuroscience*, *232*, 182–193.

Aicher, S. A., Hermes, S. M., & Hegarty, D. M. (2015). Denervation of the lacrimal gland leads to corneal hypoalgesia in a novel rat model of aqueous dry eye disease. *Investigative Ophthalmology & Visual Science*, *56*(11), 6981–6989.

Alamri, A., Bron, R., Brock, J. A., & Ivanusic, J. J. (2015). Transient receptor potential cation channel subfamily V member 1 expressing corneal sensory neurons can be subdivided into at least three subpopulations. *Frontiers in Neuroanatomy*, *9*, 71.

Almaraz, L., Manenschijn, J. A., de la Pena, E., & Viana, F. (2014). Trpm8. *Handbook of Experimental Pharmacology*, *222*, 547–579.

Altinors, D. D., Bozbeyoglu, S., Karabay, G., & Akova, Y. A. (2007). Evaluation of ocular surface changes in a rabbit dry eye model using a modified impression cytology technique. *Current Eye Research*, *32*(4), 301–307.

Ang, R. T., Dartt, D. A., & Tsubota, K. (2001). Dry eye after refractive surgery. *Current Opinion in Ophthalmology*, *12*(4), 318–322.

Bates, B. D., Mitchell, K., Keller, J. M., Chan, C. C., Swaim, W. D., Yaskovich, R., … Iadarola, M. J. (2010). Prolonged analgesic response of cornea to topical resiniferatoxin, a potent TRPV1 agonist. *Pain*, *149*(3), 522–528.

Bautista, D. M., Siemens, J., Glazer, J. M., Tsuruda, P. R., Basbaum, A. I., Stucky, C. L., … Julius, D. (2007). The menthol receptor TRPM8 is the principal detector of environmental cold. *Nature*, *448*(7150), 204–208.

Belmonte, C., Acosta, M. C., & Gallar, J. (2004). Neural basis of sensation in intact and injured corneas. *Experimental Eye Research*, *78*(3), 513–525.

Belmonte, C., Gallar, J., Pozo, M. A., & Rebollo, I. (1991). Excitation by irritant chemical substances of sensory afferent units in the cat's cornea. *The Journal of Physiology*, *437*, 709–725.

Braz, J. M., & Basbaum, A. I. (2010). Differential ATF3 expression in dorsal root ganglion neurons reveals the profile of primary afferents engaged by diverse noxious chemical stimuli. *Pain*, *150*(2), 290–301.

Carstens, E., Kuenzler, N., & Handwerker, H. O. (1998). Activation of neurons in rat trigeminal subnucleus caudalis by different irritant chemicals applied to oral or ocular mucosa. *Journal of Neurophysiology*, *80*(2), 465–492.

Caterina, M. J., & Julius, D. (2001). The vanilloid receptor: A molecular gateway to the pain pathway. *Annual Review of Neuroscience*, *24*, 487–517.

Caterina, M. J., Leffler, A., Malmberg, A. B., Martin, W. J., Trafton, J., Petersen-Zeitz, K. R., … Julius, D. (2000). Impaired nociception and pain sensation in mice lacking the capsaicin receptor. *Science*, *288*(5464), 306–313.

Caterina, M. J., Schumacher, M. A., Tominaga, M., Rosen, T. A., Levine, J. D., & Julius, D. (1997). The capsaicin receptor: A heat-activated ion channel in the pain pathway. *Nature*, *389*(6653), 816–824.

Chao, W., Belmonte, C., Benitez Del Castillo, J. M., Bron, A. J., Dua, H. S., Nichols, K. K., … Sullivan, D. A. (2016). Report of the inaugural meeting of the TFOS i(2) = initiating innovation series: Targeting the unmet need for dry eye treatment. *The Ocular Surface*, *14*(2), 264–316.

Cliff, M. A., & Green, B. G. (1994). Sensory irritation and coolness produced by menthol: Evidence for selective desensitization of irritation. *Physiology & Behavior*, *56*(5), 1021–1029.

Cruzat, A., Pavan-Langston, D., & Hamrah, P. (2010). In vivo confocal microscopy of corneal nerves: Analysis and clinical correlation. *Seminars in Ophthalmology*, *25*(5-6), 171–177.

Dvorscak, L., & Marfurt, C. F. (2008). Age-related changes in rat corneal epithelial nerve density. *Investigative Ophthalmology & Visual Science*, *49*(3), 910–916.

Dworkin, R. H. (2002). An overview of neuropathic pain: Syndromes, symptoms, signs, and several mechanisms. *The Clinical Journal of Pain*, *18*(6), 343–349.

Farazifard, R., Safarpour, F., Sheibani, V., & Javan, M. (2005). Eye-wiping test: A sensitive animal model for acute trigeminal pain studies. *Brain Research. Brain Research Protocols*, *16*(1-3), 44–49.

Faridi, U., Sisodia, B. S., Shukla, A. K., Shukla, R. K., Darokar, M. P., Dwivedi, U. N., & Shasany, A. K. (2011). Proteomics indicates modulation of tubulin polymerization by L-menthol inhibiting human epithelial colorectal adenocarcinoma cell proliferation. *Proteomics*, *11*(10), 2115–2119.

Fujita, S., Miyazono, Y., & Ohba, N. (1987). Capsaicin-induced corneal changes associated with sensory denervation in neonatal rat. *Japanese Journal of Ophthalmology*, *31*(3), 412–424.

Goswami, C., Dreger, M., Otto, H., Schwappach, B., & Hucho, F. (2006). Rapid disassembly of dynamic microtubules upon activation of the capsaicin receptor TRPV1. *Journal of Neurochemistry*, *96*(1), 254–266.

Grixti, A., Sadri, M., & Watts, M. T. (2013). Corneal protection during general anesthesia for nonocular surgery. *The Ocular Surface*, *11*(2), 109–118.

Guo, A., Vulchanova, L., Wang, J., Li, X., & Elde, R. (1999). Immunocytochemical localization of the vanilloid receptor 1 (VR1): Relationship to neuropeptides, the P2X3 purinoceptor and IB4 binding sites. *European Journal of Neuroscience*, *11*(3), 946–958.

Han, P., McDonald, H. A., Bianchi, B. R., Kouhen, R. E., Vos, M. H., Jarvis, M. F., … Moreland, R. B. (2007). Capsaicin causes protein synthesis inhibition and microtubule disassembly through TRPV1 activities both on the plasma membrane and intracellular membranes. *Biochemical Pharmacology*, *73*(10), 1635–1645.

Harti, G., Sharkey, K. A., & Pierau, F. K. (1989). Effects of capsaicin in rat and pigeon on peripheral nerves containing substance P and calcitonin gene-related peptide. *Cell and Tissue Research*, *256*(3), 465–474.

Hegarty, D. M., Hermes, S. M., Largent-Milnes, T. M., & Aicher, S. A. (2014). Capsaicin-responsive corneal afferents do not contain TRPV1 at their central terminals in trigeminal nucleus caudalis in rats. *Journal of Chemical Neuroanatomy*, *61-62*, 1–12.

Hegarty, D. M., Tonsfeldt, K., Hermes, S. M., Helfand, H., & Aicher, S. A. (2010). Differential localization of vesicular glutamate transporters and peptides in corneal afferents to trigeminal nucleus caudalis. *Journal of Comparative Neurology*, *518*(17), 3557–3569.

Hermes, S. M., Andresen, M. C., & Aicher, S. A. (2016). Localization of TRPV1 and P2X3 in unmyelinated and myelinated vagal afferents in the rat. *Journal of Chemical Neuroanatomy*, *72*, 1–7.

Hirata, H., & Meng, I. D. (2010). Cold-sensitive corneal afferents respond to a variety of ocular stimuli central to tear production: Implications for dry eye disease. *Investigative Ophthalmology & Visual Science*, *51*(8), 3969–3976.

Hirata, H., Mizerska, K., Marfurt, C. F., & Rosenblatt, M. I. (2015). Hyperosmolar tears induce functional and structural alterations of corneal nerves: Electrophysiological and anatomical evidence toward neurotoxicity. *Investigative Ophthalmology & Visual Science*, *56*(13), 8125–8140.

Hiura, A., & Nakagawa, H. (2012). Innervation of TRPV1-, PGP-, and CGRP-immunoreactive nerve fibers in the subepithelial layer of a whole mount preparation of the rat cornea. *Okajimas Folia Anatomica Japonica*, *89*(2), 47–50.

Ivanusic, J. J., Wood, R. J., & Brock, J. A. (2013). Sensory and sympathetic innervation of the mouse and guinea pig corneal epithelium. *Journal of Comparative Neurology*, *521*(4), 877–893.

Jones, M. A., & Marfurt, C. F. (1991). Calcitonin gene-related peptide and corneal innervation: A developmental study in the rat. *Journal of Comparative Neurology*, *313*(1), 132–150.

Jones, M. A., & Marfurt, C. F. (1998). Peptidergic innervation of the rat cornea. *Experimental Eye Research*, *66*(4), 421–435.

Kallinikos, P., Berhanu, M., O'Donnell, C., Boulton, A. J., Efron, N., & Malik, R. A. (2004). Corneal nerve tortuosity in diabetic patients with neuropathy. *Investigative Ophthalmology & Visual Science*, *45*(2), 418–422.

Kapitein, L. C., & Hoogenraad, C. C. (2015). Building the neuronal microtubule cytoskeleton. *Neuron*, *87*(3), 492–506.

Kijpornyongpan, T., Sereemaspun, A., & Chanchao, C. (2014). Dose-dependent cytotoxic effects of menthol on human malignant melanoma A-375 cells: Correlation with TRPM8 transcript expression. *Asian Pacific Journal of Cancer Prevention*, *15*(4), 1551–1556.

Klein, A., Carstens, M. I., & Carstens, E. (2011). Facial injections of pruritogens or algogens elicit distinct behavior responses in rats and excite overlapping populations of primary sensory and trigeminal subnucleus caudalis neurons. *Journal of Neurophysiology*, *106*(3), 1078–1088.

Ko, J. A., Mizuno, Y., Ohki, C., Chikama, T., Sonoda, K. H., & Kiuchi, Y. (2014). Neuropeptides released from trigeminal neurons promote the stratification of human corneal epithelial cells. *Investigative Ophthalmology & Visual Science*, *55*(1), 125–133.

Kurose, M., & Meng, I. D. (2013). Dry eye modifies the thermal and menthol responses in rat corneal primary afferent cool cells. *Journal of Neurophysiology*, *110*(2), 495–504.

Lambiase, A., Aloe, L., Mantelli, F., Sacchetti, M., Perrella, E., Bianchi, P., … Bonini, S. (2012). Capsaicin-induced corneal sensory denervation and healing impairment are reversed by NGF treatment. *Investigative Ophthalmology & Visual Science*, *53*(13), 8280–8287.

Lee, M. K., Rebhun, L. I., & Frankfurter, A. (1990). Posttranslational modification of class III beta-tubulin. *Proceedings of the National Academy of Sciences of the United States of America*, *87*(18), 7195–7199.

Lemp, M. A. (2008). Advances in understanding and managing dry eye disease. *American Journal of Ophthalmology*, *146*(3), 350–356.

Li, Q., Wang, X., Yang, Z., Wang, B., & Li, S. (2009). Menthol induces cell death via the TRPM8 channel in the human bladder cancer cell line T24. *Oncology*, *77*(6), 335–341.

Lischka, F. W., Gomez, G., Yee, K. K., Dankulich-Nagrudny, L., Lo, L., Haskins, M. E., & Rawson, N. E. (2008). Altered olfactory epithelial structure and function in feline models of mucopolysaccharidoses I and VI. *Journal of Comparative Neurology*, *511*(3), 360–372.

Liu, H., Begley, C., Chen, M., Bradley, A., Bonanno, J., McNamara, N. A., … Simpson, T. (2009). A link between tear instability and hyperosmolarity in dry eye. *Investigative Ophthalmology & Visual Science*, *50*(8), 3671–3679.

Lolignier, S., Gkika, D., Andersson, D., Leipold, E., Vetter, I., Viana, F., … Busserolles, J. (2016). New insight in cold pain: Role of ion channels, modulation, and clinical perspectives. *Journal of Neuroscience*, *36*(45), 11435–11439.

Lu, H. F., Hsueh, S. C., Yu, F. S., Yang, J. S., Tang, N. Y., Chen, S. C., & Chung, J. G. (2006). The role of Ca2 + in (-)-menthol-induced human promyelocytic leukemia HL-60 cell death. *In Vivo*, *20*(1), 69–75.

Lu, H. F., Liu, J. Y., Hsueh, S. C., Yang, Y. Y., Yang, J. S., Tan, T. W., … Chung, J. G. (2007). (-)-Menthol inhibits WEHI-3 leukemia cells in vitro and in vivo. *In Vivo*, *21*(2), 285–289.

Madrid, R., Donovan-Rodriguez, T., Meseguer, V., Acosta, M. C., Belmonte, C., & Viana, F. (2006). Contribution of TRPM8 channels to cold transduction in primary sensory neurons and peripheral nerve terminals. *Journal of Neuroscience*, *26*(48), 12512–12525.

Mantyh, P. W., Allen, C. J., Ghilardi, J. R., Rogers, S. D., Mantyh, C. R., Liu, H., … Maggio, J. E. (1995). Rapid endocytosis of a G protein-coupled receptor: Substance P evoked internalization of its receptor in the rat striatum in vivo. *Proceedings of the National Academy of Sciences of the United States of America*, *92*(7), 2622–2626.

Marfurt, C. F., & Del Toro, D. R. (1987). Corneal sensory pathway in the rat: A horseradish peroxidase tracing study. *Journal of Comparative Neurology*, *261*(3), 450–459.

Marfurt, C. F., Ellis, L. C., & Jones, M. A. (1993). Sensory and sympathetic nerve sprouting in the rat cornea following neonatal administration of capsaicin. *Somatosensory & Motor Research*, *10*(4), 377–398.

McKemy, D. D., Neuhausser, W. M., & Julius, D. (2002). Identification of a cold receptor reveals a general role for TRP channels in thermosensation. *Nature*, *416*(6876), 52–58.

Meng, I. D., & Bereiter, D. A. (1996). Differential distribution of Fos-like immunoreactivity in the spinal trigeminal nucleus after noxious and innocuous thermal and chemical stimulation of rat cornea. *Neuroscience*, *72*(1), 243–254.

Muller, L. J., Marfurt, C. F., Kruse, F., & Tervo, T. M. (2003). Corneal nerves: Structure, contents and function. *Experimental Eye Research*, *76*(5), 521–542.

Murata, Y., & Masuko, S. (2006). Peripheral and central distribution of TRPV1, substance P and CGRP of rat corneal neurons. *Brain Research*, *1085*(1), 87–94.

Nakagawa, H., Hiura, A., Mitome, M., & Ishimura, K. (2009). Nerve fibers that were not stained with the non-specific acetylcholinesterase (NsAchE) method, and TRPV1- and IB4-positive nerve fibers in the rat cornea. *Journal of Medical Investigation*, *56*(3-4), 157–165.

Neubert, J. K., King, C., Malphurs, W., Wong, F., Weaver, J. P., Jenkins, A. C., … Caudle, R. M. (2008). Characterization of mouse orofacial pain and the effects of lesioning TRPV1-expressing neurons on operant behavior. *Molecular Pain*, *4*, 43.

Ogilvy, C. S., & Borges, L. F. (1990). Changes in corneal innervation during postnatal development in normal rats and in rats treated at birth with capsaicin. *Investigative Ophthalmology & Visual Science*, *31*(9), 1810–1815.

Parra, A., Gonzalez-Gonzalez, O., Gallar, J., & Belmonte, C. (2014). Tear fluid hyperosmolality increases nerve impulse activity of cold thermoreceptor endings of the cornea. *Pain*, *155*(8), 1481–1491.

Parra, A., Madrid, R., Echevarria, D., del Olmo, S., Morenilla-Palao, C., Acosta, M. C., … Belmonte, C. (2010). Ocular surface wetness is regulated by TRPM8-dependent cold thermoreceptors of the cornea. *Nature Medicine*, *16*(12), 1396–1399.

Patapoutian, A., Tate, S., & Woolf, C. J. (2009). Transient receptor potential channels: Targeting pain at the source. *Nature Reviews Drug Discovery*, *8*(1), 55–68.

Quallo, T., Vastani, N., Horridge, E., Gentry, C., Parra, A., Moss, S., … Bevan, S. (2015). TRPM8 is a neuronal osmosensor that regulates eye blinking in mice. *Nature Communications*, *6*, 7150.

Robbins, A., Kurose, M., Winterson, B. J., & Meng, I. D. (2012). Menthol activation of corneal cool cells induces TRPM8-mediated lacrimation but not nociceptive responses in rodents. *Investigative Ophthalmology & Visual Science*, *53*(11), 7034–7042.

Shaheen, B. S., Bakir, M., & Jain, S. (2014). Corneal nerves in health and disease. *Survey of Ophthalmology*, *59*(3), 263–285.

Shimada, S. G., & LaMotte, R. H. (2008). Behavioral differentiation between itch and pain in mouse. *Pain*, *139*(3), 681–687.

Szolcsanyi, J., Jancso-Gabor, A., & Joo, F. (1975). Functional and fine structural characteristics of the sensory neuron blocking effect of capsaicin. *Naunyn-Schmiedeberg's Archives of Pharmacology*, *287*(2), 157–169.

Takashima, Y., Daniels, R. L., Knowlton, W., Teng, J., Liman, E. R., & McKemy, D. D. (2007). Diversity in the neural circuitry of cold sensing revealed by genetic axonal labeling of transient receptor potential melastatin 8 neurons. *Journal of Neuroscience*, *27*(51), 14147–14157.

Tang-Schomer, M. D., Patel, A. R., Baas, P. W., & Smith, D. H. (2010). Mechanical breaking of microtubules in axons during dynamic stretch injury underlies delayed elasticity, microtubule disassembly, and axon degeneration. *The FASEB Journal*, *24*(5), 1401–1410.

Theophanous, C., Jacobs, D. S., & Hamrah, P. (2015). Corneal neuralgia after LASIK. *Optometry and Vision Science*, *92*(9), e233–e240.

Tran, M. T., Ritchie, M. H., Lausch, R. N., & Oakes, J. E. (2000). Calcitonin gene-related peptide induces IL-8 synthesis in human corneal epithelial cells. *Journal of Immunology*, *164*(8), 4307–4312.

Tuisku, I. S., Konttinen, Y. T., Konttinen, L. M., & Tervo, T. M. (2008). Alterations in corneal sensitivity and nerve morphology in patients with primary Sjogren's syndrome. *Experimental Eye Research*, *86*(6), 879–885.

Vesaluoma, M., Muller, L., Gallar, J., Lambiase, A., Moilanen, J., Hack, T., … Tervo, T. (2000). Effects of oleoresin capsicum pepper spray on human corneal morphology and sensitivity. *Investigative Ophthalmology & Visual Science*, *41*(8), 2138–2147.

Wasner, G., Schattschneider, J., Binder, A., & Baron, R. (2004). Topical menthol–a human model for cold pain by activation and sensitization of C nociceptors. *Brain*, *127*(Pt 5), 1159–1171.

Xing, H., Ling, J., Chen, M., & Gu, J. G. (2006). Chemical and cold sensitivity of two distinct populations of TRPM8-expressing somatosensory neurons. *Journal of Neurophysiology*, *95*(2), 1221–1230.

Zaelzer, C., Hua, P., Prager-Khoutorsky, M., Ciura, S., Voisin, D. L., Liedtke, W., & Bourque, C. W. (2015). ΔN-TRPV1: A molecular co-detector of body temperature and osmotic stress. *Cell Reports*, *13*(1), 23–30.

Zhou, Y., Zhang, M., Sun, G. Y., Liu, Y. P., Ran, W. Z., Peng, L., & Guan, C. X. (2013). Calcitonin gene-related peptide promotes the wound healing of human bronchial epithelial cells via PKC and MAPK pathways. *Regulatory Peptides*, *184*, 22–29.

How to cite this article: Hegarty DM, Hermes SM, Yang K, Aicher SA. Select noxious stimuli induce changes on corneal nerve morphology. *J. Comp. Neurol.* 2017;525:2019–2031. https://doi.org/10.1002/cne.24191